



Direct-Deposition to Create High Particle Loading Propellants with Controlled Architecture: Combustion And Mechanical Properties

Tao Wu¹, Xiangyu Li², Xiuli, Hu², Jeffery B. Delisio¹, Wenbo Zhou³, and Michael R. Zachariah^{4*}
 University of Maryland, College Park, MD 20742

*Corresponding author: mrz@umd.edu

One of the challenges in the use of energetic nanoparticles within a polymer matrix for propellant application is obtaining high particle loading while maintaining mechanical integrity and reactivity. In this study, an electrospray deposition technique was employed to increase particle loading of nano aluminum in a thermite film and demonstrate the potential of a fluoropolymer, polyvinylidene fluoride (PVDF), as an energetic binder. In addition, multilayer films contain alternating layers of Al/PVDF thermite layers and spacer layers of PVDF were prepared by a layer-by-layer deposition method. A mass percentage of 55% nano Al in PVDF was determined to have the best combustion performance among all the single layer films. And the reactive properties of multilayer films significantly outperformed the single-layer films.

I. Introduction

DUE to its high energy density and high energy release rate during oxidation, aluminum, one kind of micro sized metal particles, has been broadly used as an important component in solid rocket propellants.^{1,2} Compared to micro size aluminum which has gain a great deal of attention, the nanosized aluminum owns better properties, such as lower ignition temperature and fast burn rates resulting from its enhanced surface area.^{3,4} Normally, a polymer is often used to incorporate the fuel and oxidizer particles in order to give the fuel mechanical integrity and also participate in a favorable manner in the overall energy release chemistry.^{5,6,7} Various binders have been employed such as epoxy, nitrocellulose, and fluorine-containing polymers.^{8,9,10} Among all of the binders, fluorine-containing binders offer a delivery method for a very strong oxidizer due to the strong oxidation potential of fluorine and the high heat of reaction to form aluminum fluoride (AlF₃).^{11,12} To be noticed, the formation of AlF₃ releases about 80% more energy per unit mass than oxidation of aluminum.¹³ As a binder, the polymer involved in solid propellants should not only possess high energy release but also certain solubility in solvents. In this case, polyvinylidene fluoride (PVDF) has been widely used as a binder due to its high mechanical strength, excellent thermal stability, and chemical resistance, and good solubility in polar solvents, such as acetone, dimethyl sulfoxide, and dimethyl-formamide (DMF).¹⁴ Here, we have employed it as the oxidizer and reactive binder for aluminum.

Electrospray deposition has been considered as an effective means for the deposition of thin films.¹⁵ In the electrospray process, aerosol droplets can be ejected from a liquid surface by applying a high electric field to overcome the surface tension and the intermolecular forces at the solution interface. The generated droplets will undergo Coulombic explosion via a “droplet fission” process and lead to a very narrow drop size distribution, which is unable to obtain by other methods.¹⁶ The charged droplets can be readily directed to a substrate to create a thin film. The electrospray method can conveniently control the thickness, morphology, and uniformity of a film by simply adjusting the solution concentration, flow rate, and applied voltage. Above all, the process is performed at ambient temperature under atmosphere pressure.

¹ Graduate Research Assistant, Chemistry and Biochemistry, 0107 Chemistry Building.

² Visiting Researcher, Nanjin University of Science and Technology, Nanjing 210094, China.

³ Graduate Research Assistant, Chemical and Biomolecular Engineering, 2113 Chemical and Nuclear Engineering Building.

⁴ Professor, Chemical and Biomolecular Engineering and Chemistry and Biochemistry, 2113 Chemical and Nuclear Engineering Building.

In this work we employ a laminate structure to enhance both the reactive and structural properties of the energetic propellant. The fuel/oxidizer solids to be explored are drawn from the class of nanothermites that are highly reactive and which can lead to as much as 1000x enhancement in reactivity as compared to their micron counterparts. To create the laminate structure we build on prior work in the use of electro-spray deposition as a simple method to fabricate nano-composites with high nanoparticle loadings. The laminate is composed of alternating layers of aluminum nanopowders/copper oxide nanopowders thermites in a polyvinylidene fluoride (PVDF) reactive binder, with a spacer layer of PVDF. These results show that enhancement in both the reactive and mechanical property are found in laminate films.

In addition, an energetic fiber reinforced composite was employed to enhance both the reactive and structural properties of the energetic propellant. To create a fiber reinforced films we build on prior work in the use of electro-spray deposition as a simple method to fabricate nano-composites with high nanoparticle loadings.^[32] The fiber reinforced films are composed of Al-NPs/CuO-NPs thermites in a PVDF reactive binder, with PVDF nanofibers embedded within. These results show that enhancement in both the reactive and mechanical property are found in fiber reinforced films.

II. Experimental

A. Materials

Aluminum nanopowders (Al-NPs) (ALEX, 50 nm) were purchased from Argonide Corporation and tested by thermogravimetric methods to determine the active Al content as ~70% by mass. Copper oxide nanopowders (CuO-NPs) (99.8 wt%, ~30nm), Ammonium perchlorate (AP) (99.8 wt%), Polyvinylidene fluoride (PVDF) (Mw = 534.000) and Dimethylformamide (DMF) (99.8 wt%) were purchased from Sigma–Aldrich.

B. Precursors Preparation

For a typical fabricating process, (a laminate Al/CuO thermite (PVDF as binder) – PVDF film) , 400 mg of PVDF was dissolved in 6 ml DMF to create the precursor for the PVDF layer. The precursor used forming the Al/CuO thermite layer in double layer and laminate films included 300 mg of PVDF dissolved in 6 ml DMF, to which. 408 mg of Al-NPs, 531 mg of CuO-NPs was dispersed into the PVDF/DMF solution. In addition we found that a small quantity 18 mg of AP was useful in stabilizing the electrospray to create a crack free thermite layer. The mixture was stirred vigorously for 30 minutes, and ultrasonically mixed for 60 min to allow the nanoparticles to disperse homogeneously. This was followed by an additional 24 hours of magnetic stirring at room temperature.

C. Film Deposition

As presented in Figure 1, films were deposited using electrospray methods previous used by our group.^{17,18} Electrospray of pure PVDF and the thermite mixture could be alternated by the use of a dual spray setup. For this work we employed 0.023 mm ID stainless tubing for the ES injector which were fed by a syringe pump operating at 2 ml/hr. A rotating collector held at a ground potential was used to collect the laminate film. The jet-to-substrate distance was held at 6 cm, and was chosen empirically so as to enable a wide spray pattern, and sufficient time to evaporate the solvent so as not to have visible pooling of liquid on the substrate. A linear field strength operated in the range of ~2-3 kV/cm resulted in a stable cone-jet mode, and was the nominal operating condition. The thickness of each layer can be easily adjusted by the duration of the electrospray deposition.

For fiber reinforced composites, we employed a two-needle spray setup of which two 0.023 mm ID stainless tubing for the ES injector were fed by individual syringe pumps. A rotating collector held at ground potential was used to collect the fiber reinforced film. The jet-to-substrate distance was 10 cm and 6 cm for the electrospinning and electrospray, respectively. The same working voltage of 18 kV was applied for both of electrospinning and electrospray. In the experiment, fine droplets from electrospray were deposited wet to form the matrix, and nanofibers from electrospinning was collected dry as the reinforcement. Flow rate of electrospray process was adjusted accordingly to vary the matrix mass loading of the film.

D. Characterization

The reactive behavior of the thermite laminate film was characterized by the propagation velocity using a high speed camera (Phantom v12.0) with a frame rate of 7000 frames per second. The as prepared films had sufficient mechanical strength to be easily removed from the substrate backing, and was cut to a 3 cm x0.5 cm section. All combustion tests were carried out in argon, and ignited at one end by a hot Ni-Cr wire. Each sample was tested in triplicate to obtain the average combustion propagation velocity.

Scanning electron microscopy (SEM, Hitachi, SU-70 FEG-SEM) equipped with energy dispersive X-ray spectroscopy (EDS) was used to characterize the morphologies and thickness of the laminate film. The film was cut into narrow strips (~1 mm width) and then fractured in liquid nitrogen to obtain a flat and uniform fracture section for the cross-section image. All samples were sputter coated with carbon prior to imaging.

The mechanical properties of the laminate film were obtained by a home-made micro-tensile tester [33]. Three Strip specimens (2.5 cm × 0.5cm) were tested for each film. The quasi-static loading strain rate of 10^{-4} s^{-1} was applied by a customized Pico motor control software. A video extensometer was used to acquire the strain data in the gage section of the specimen. The load data from the load cell is obtained with Correlated Solutions (Columbia, SC) Vic-Gauge 2006 software. Before the test the initial thickness was obtained by the SEM and width of the film was carefully measured by a digital caliper.

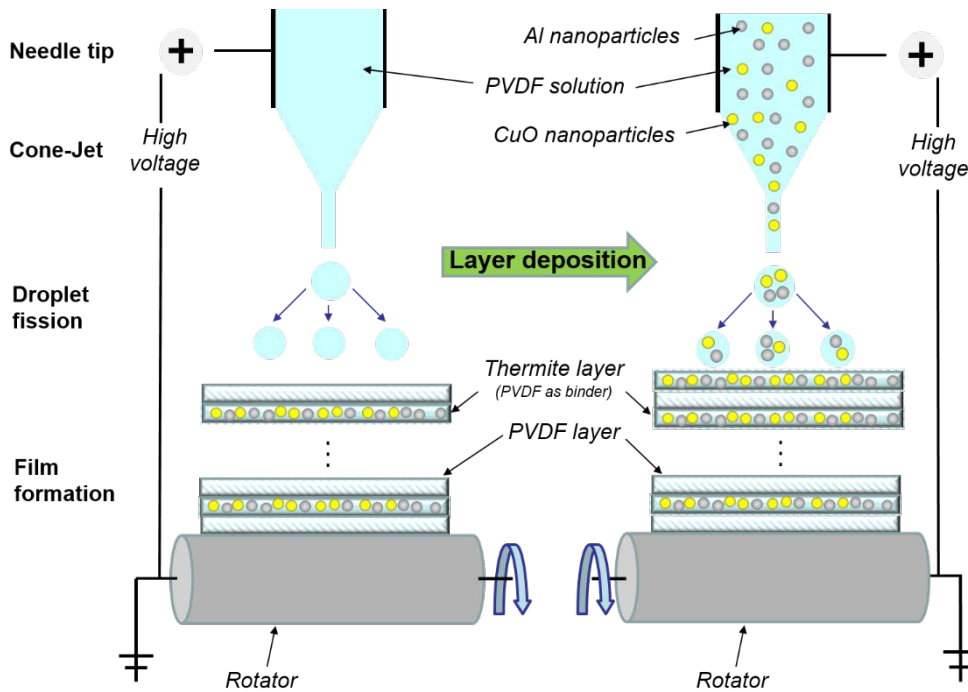


Figure 1. Illustration of electro-spray deposition process for fabricating laminate Al/CuO/PVDF thermite – PVDF films.

III. Results and Discussion

A. Laminate Films.

Figure 2 shows SEM and EDS images of the deposited films. The standalone PVDF film, (Figure 2a and b) shows a crack free, smooth and uniform polymer film. However, the standalone Al/CuO/PVDF film (Figure 2c), as would be expected, shows a much rougher fracture surface but still maintained a uniform thickness. Under high magnification (Figure 2d) one can see that the PVDF is forming a fibrous polymer network connecting, and enveloping the nanoparticles. EDS mapping (Figure 2g-j) indicates that some aggregation of the nanoparticles is occurring. Finally we can see that alternating the spray precursors leads to a well-defined laminate film (Figure 2e), with considerable lateral conformity and thickness, and the layers appear to be conformal at the interfaces (Figure 1f). We find no clear distinction in morphology between the laminate structure and the standalone films.

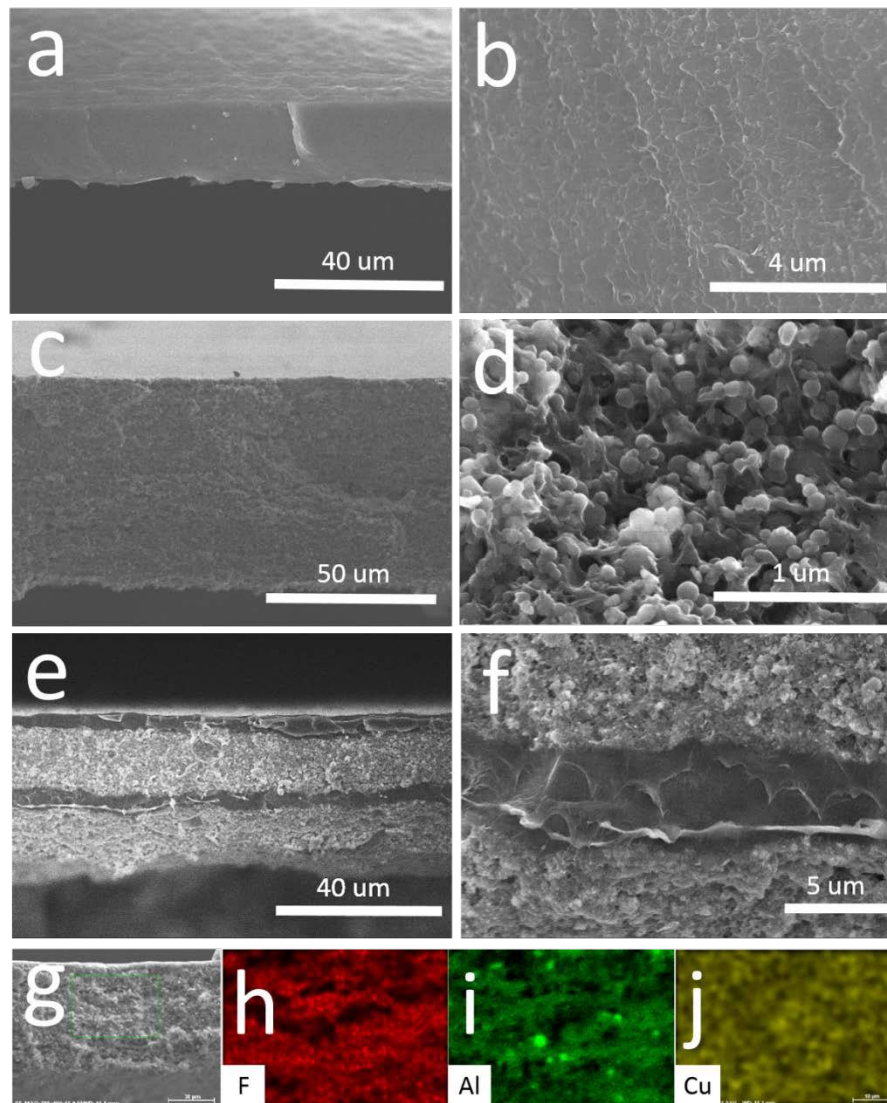


Figure 2. a-j) Cross-sectioned SEM images (a) and (b) PVDF film; (c) and (d) Al/CuO/PVDF thermite film; (e) 4 layer laminate film; interfacial area (f); EDS image of Al/CuO/PVDF thermite film (g-j).

To compare the reactive properties for both single and layer films, we prepared single and double layer films of the same total composition, but with a different spatial arrangement. First the double layer films was fabricated with fixed thermite layer thickness, but different PVDF layer thickness, and for which the thermite layer was fixed at 10 μm . In all cases the component concentrations in the thermite were held at 24 wt% PVDF, 33 wt% Al, and 43 wt% CuO in the thermite layer. Ranging from 0 to 87 wt% the mass ratio of PVDF in the whole film is increasing while the PVDF layer becomes thicker. As such in this experiment the thermite layer always has the same solids loading. For each double layer film, a single layer film with same composition was also prepared. The thermite layer thickness, PVDF layer thickness, PVDF mass ratio and the stoichiometry of the whole film of as-prepared double and single layer films are summarized in Table 1.

Table 1. Thermite and PVDF layer thickness, PVDF mass ratio and stoichiometry of the whole film of as-prepared double and single layer films

Double-layer films			
PVDF mass ratio (%)	Molar ratio PVDF/Al/CuO	Thermite layer thickness (μm)	PVDF layer Thickness (μm)
24	0.5/1.1/0.7	10	0
38	1.0/1.1/0.7	10	2.5
51	1.6/1.1/0.7	10	5
76	2.8/1.1/0.7	10	20
87	10.5/1.1/0.7	10	45

Single-layer films	
PVDF mass ratio (%)	Molar ratio PVDF/Al/CuO
24	0.5/1.1/0.7
38	1.0/1.1/0.7
51	1.6/1.1/0.7
76	2.8/1.1/0.7
87	10.5/1.1/0.7

All the films above could be ignited easily and showed a self-sustaining stable propagating combustion. Figure 3 shows the average combustion propagation velocity of the double layer, and corresponding single layer films with different PVDF mass ratio in argon. For both single and double layer films, the molar ratio of PVDF, is increasing from point a to point h and i. The stoichiometric composition (PVDF mass ratio 38 wt%), point c (becomes lean with increasing PVDF) shows the fastest propagation velocity in argon for the single layer films. For the double layer, the fastest propagation velocity occurs at a PVDF mass ratio of 51 wt% (point d), and thus is stoichiometrically fuel lean. This can be understood as requiring extra oxidizer over stoichiometric because of the spatial separation in the two layer film, relative to the single layer case. A possible mechanisms of the reactive behavior could be that when the PVDF is below 51 wt%, the combustion propagation velocity is decreasing probably due to the lack of PVDF to enhance all of the thermite layer. Above 51 wt%, not all of the thermite layer can be enhanced due to the decomposition of unreacted PVDF which acts as a heat sink. Importantly however, all double layer films demonstrate a higher combustion propagation velocity than the corresponding single layer film.

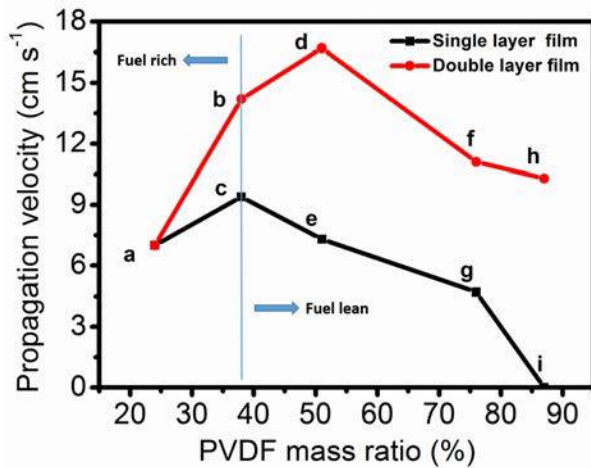


Figure 3. Average propagation velocity of double and single layer thermite film as a function of PVDF mass ratio, when the thermite layer thickness is fixed at 10 μm in double layer thermite film. Particle concentration in thermite layer is fixed in double layer thermite films.

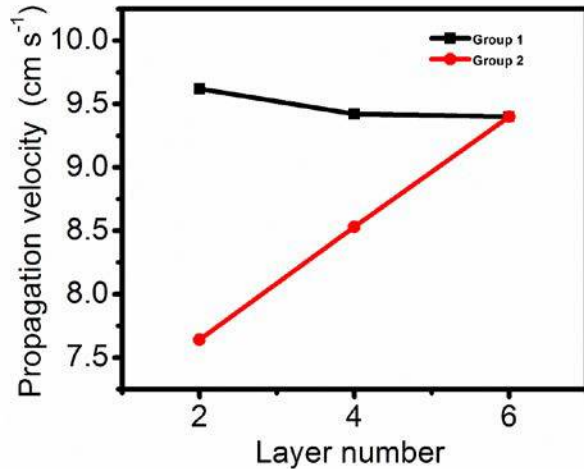


Figure 4. Average combustion propagation velocity of laminate film sample group 1 and 2. In group 1, all the PVDF layers were fixed at 7 m, and the thermite layers were fixed at 30 μm , In group 2, the thickness ratio of the thermite layer and the PVDF spacer layer is 30/7 in each laminate film with the same total film thickness of 111 μm , thus, as we increase the number of layers, the absolute layer thickness decreases.

Next we turn to multilayer films as they are ultimately how a formulated propellant may be built-up. PVDF layers and thermite layers were deposited alternately in all laminate films. Thermite layers in the laminate films contain 24 wt% PVDF, 33 wt% Al and 43 wt% CuO. Two groups of samples were prepared, consisting of 2, 4 and 6 layers. In group 1, all the PVDF layers were fixed at $7\ \mu\text{m}$, and the thermite layers at $30\ \mu\text{m}$. The thickness ratio of thermite layer and PVDF spacer layer were fixed at 30/7 in each laminate film of group 2, with the same total film thickness of $111\ \mu\text{m}$. All samples in the two groups have the same material composition of 39 wt% PVDF, 26 wt% Al and 35 wt% CuO since they have the same thermite / PVDF layer thickness ratio. The laminate films with 6 layers in both groups are actually the same film. Figure 4 demonstrates the combustion propagation velocity of the two groups of samples. For group 1, the combustion propagation velocity of the films shows no obvious difference, with an increase in number of layers. This is not surprising, as we should not expect any significant cooperative effect of stacking multiple layers. It also implies that a large structure on the length scale of a rocket motor could be fabricated using this approach. On the other hand, group 2, which consists of laminates with a fixed total thickness, clearly show propagation velocity enhancement as the bi-layer spacing is decreased.

Our conceptual model to explain the observation that decreasing the layer thickness enhances the reaction velocity may be considered in the following way. The thermite layer will obviously on its own have a faster propagation velocity than the PVDF spacer layer. As such one can imagine that the spacer layer erosion rate will lag behind due to the heat flux, q , needed to decompose and release this layer. Since the thermite layer is fuel rich, as the PVDF layer is heated it can participate in the reaction by transporting oxidizer, m , into the post-reaction region (Figure 5a). Decreasing the spacing decreases the effective path length for transport of oxidizer species to complete the reaction and thus enhances the propagation speed (Figure 5b). By decreasing the spacing therefore between the thermite and PVDF layer, we should, and we do in fact see enhanced propagation as shown in group 2 in Figure 5.

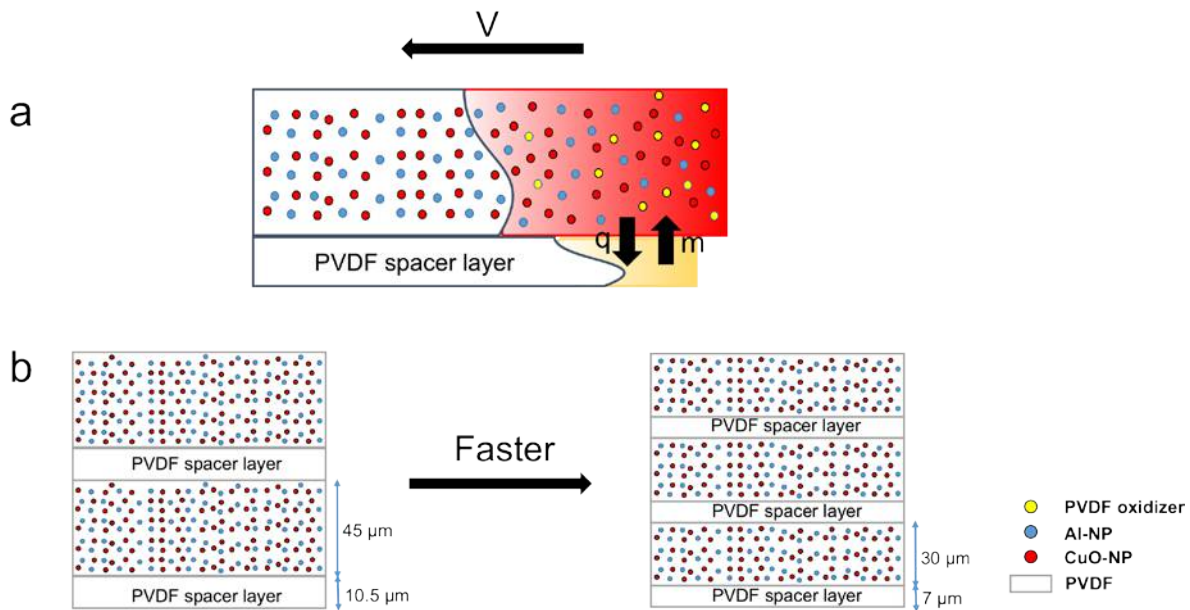


Figure 5. Conceptual model of the reaction mechanism between the thermite layer and PVDF layer of 2 layers laminate film (a). Decreasing the spacing between the thermite and PVDF layers enhances the propagation speed of the film (b).

Figure 6 shows the stress-strain behavior of the three structures, and demonstrates that the laminate (film 2) greatly outperformed the same structure without the spacer layer (film 3). The tensile strength of the laminate showed a ~62 % improvement over both the corresponding single layer, and the dispersed particle layer (film 3). The laminate has the strain of 58%, which is considerably better than the corresponding 0.91% for the dispersed structure film 3, and dropped to 0.76% for the thermite/PVDF film 1. Similarly, the toughness of the laminate is a factor of 5 higher than film 3, and 38 times larger than film 1. Thus we can conclude that a laminate structure uniformly improves the mechanical properties of high loading particle systems.

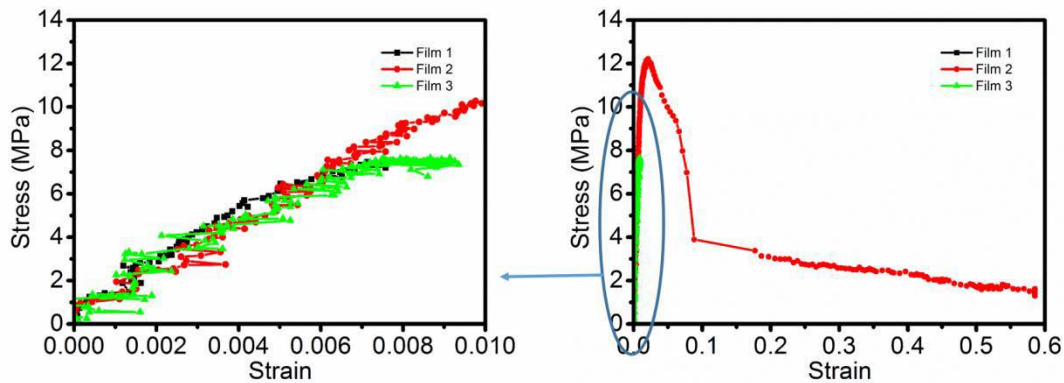


Figure 6. Stress–strain curves of film 1 (Green), 2 (Black) and 3 (Red). Film 1: Thermite /PVDF; Film 2: Film 1 with additional PVDF spacer layers to create a 6 layer film; Film 3: Film 2 but with the thermite particles dispersed evenly.

B. Fiber Reinforced Films.

Figure 7 shows SEM images of the deposited fibers and films. The standalone PVDF/Al-NPs/CuO-NPs thermite film (The matrix, Figure 7a) shows a crack free, rough, but thickness uniform polymer film. Under high magnification (Figure 7b) one can see that the PVDF binder forms a fibrous polymer network connecting, and enveloping the nanoparticles. Figure 7c is the fracture section of the fiber reinforced film which contains 21.1% PVDF nanofiber (40 wt% total PVDF, average fiber diameter 110 nm). The nanofibers protrude out from the fracture section of the dense thermite film indicates that those films were embedded within the thermite matrix (Figure 7d).

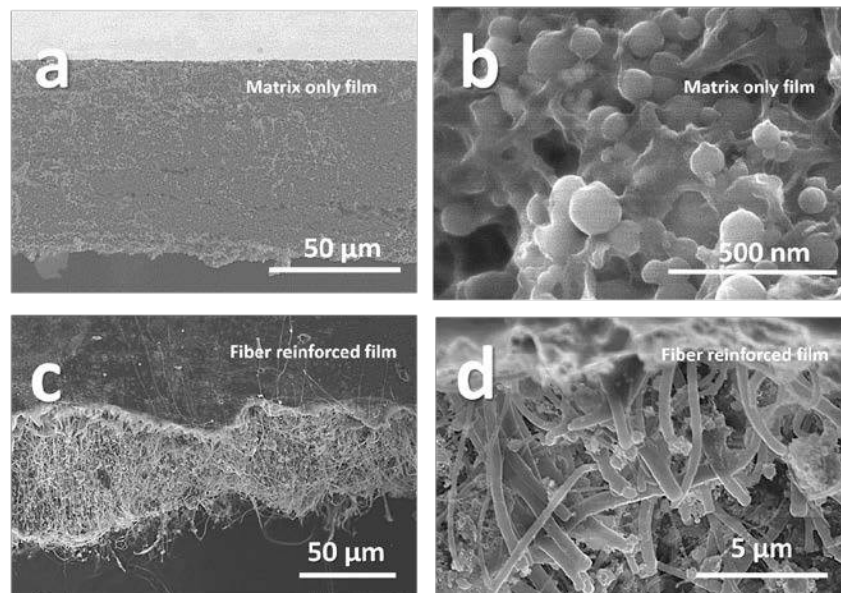


Figure 7. Cross-sectioned SEM images (a) and (b) of PVDF/Al-NPs/CuO-NPs thermite matrix only film; (c) and (d) fracture section of the fiber reinforced film (21.1 wt% PVDF nanofiber, average fiber diameter 110 nm).

Figure 8 shows the average combustion propagation velocity of the fiber reinforced, and corresponding non-nanofiber films with different total PVDF mass ratio in argon. The left most data point corresponding to zero PVDF nanofiber, is actually just a thermite matrix only film. Both types of films follow the same basic trend. The burning rate of both the fiber reinforced and corresponding non-nanofiber film increases to a PVDF mass ratio of 40 wt%. For both fiber reinforced and non-nanofiber films, the molar ratio of PVDF is increasing. The films with 40 wt% total PVDF shows the fastest propagation velocity in argon for both films. This can be understood as it has the

component most close to the stoichiometry composition (Table 1). Meanwhile, all fiber reinforced films demonstrate a higher combustion propagation velocity than the corresponding non-nanofiber films.

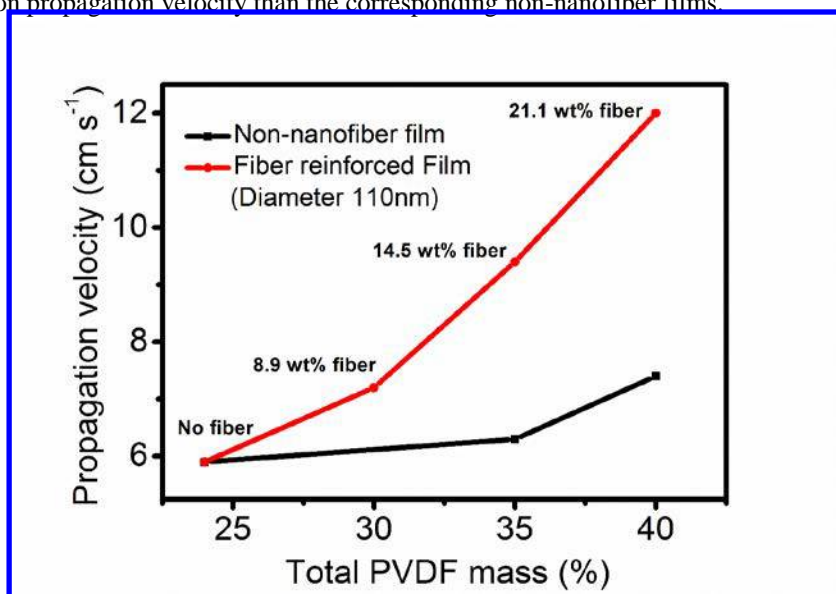


Figure 8. Average propagation velocity of fiber reinforced and single layer thermite film as a function of PVDF mass (including PVDF in fibers), when the PVDF nanofiber diameter is fixed at 110 nm. Particle concentration in matrix is fixed in all fiber reinforced films.

IV. Conclusion

A direct deposition process is demonstrated to create laminate nanothermite-based energetic polymer films and PVDF nanofiber reinforced nanothermite-based energetic polymer films. These structures show enhanced performance, with combustion propagation velocity correlated with decreasing layer separation and adding PVDF fibers into energetic films. The mechanical properties of laminate films is far superior to single layer films and demonstrate that high metal loadings can be achieved using this laminate structure.

Acknowledgments

This work was financially supported by ARO, DTRA and AFOSR. We acknowledge the support of the Maryland Nanocenter and its AimLab.

References

- ¹Sullivan, K., Young, G., Zachariah, M.R., "Enhanced reactivity of nano-B/Al/CuO MIC's," *Combust. Flame*, Vol. 156, 2009, pp. 302-309.
- ²Yetter, R. A., Risha, G. A., Son, S. F., "Metal particle combustion and nanotechnology," *P. Combust. Inst.* Vol. 32, 2009, pp. 1819-1838.
- ³Meda, L., Marra, G., Galfetti, L., Severini, F., De Luca, L., "Nano-aluminum as energetic material for rocket propellants," *Mat. Sci. Eng. C*. Vol. 27, 2007, pp. 1393-1396.
- ⁴Jian, G., Feng, J., Jacob, R. J., Egan, G. C., Zachariah, M. R., "Super - reactive Nanoenergetic Gas Generators Based on Periodate Salts," *Angew. Chem. Int. Ed.* Vol. 52, 2013, pp. 9743-9746.
- ⁵Sadeghipour S., Ghaderian J., Wahid M., "Advances in aluminum powder usage as an energetic material and applications for rocket Propellant," presented at *The 4th International Meeting of Advances in Thermalfluids (IMAT 2011)*, 2012.
- ⁶Yan, S., Jian, G. Q., Zachariah, M. R., "Electrospun nanofiber-based thermite textiles and their reactive properties," *ACS Appl. Mater. Interf.* Vol. 12, 2012, pp. 6432-6435.
- ⁷Gromov, A. A., Teipel, U., *Metal Nanopowders: Production, Characterization, and Energetic Applications*, Wiley, 2014.
- ⁸Parthiban, S., Raganandan, B., Jain, S. R., "Interpenetrating polymer networks as binders for solid composite propellants," *Defence Sci. J.* Vol. 42, 2013, pp. 147-156.

⁹Miller, H. A., Kusel, B. S., Danielson, S. T., Neat, J. W., Avjian, E. K., Pierson, S. N., Budy, S. M., Ball, D. W., Iacono, S. T., Kettwich, S. C., "Metastable nanostructured metallized fluoropolymer composites for energetics," *J. Mater. Chem. A* Vol. 1, 2013, pp. 7050-7058.

¹⁰Li, X., Liu, X., Cheng, Y., Li, Y., Mei, X., "Thermal decomposition properties of double-base propellant and ammonium perchlorate," *J. Therm. Anal. Calorim.* Vol. 115, 2014, pp. 887-894.

¹¹Smith, D. W., Iacono, S. T., Boday, D. J., Kettwich, S. C., *Advances in Fluorine-Containing Polymers*, American Chemical Society, 2012.

¹²Koch, E. C., *Metal-Fluorocarbon Based Energetic Materials*, Wiley-VCH Verlag GmbH & Co. KGaA, Weinheim, Germany 2012.

¹³Lide, D. R., *77th CRC Handbook of Chemistry and Physics*, CRC Press, Boca Raton, Florida 1996.

¹⁴Wang, Y., Travas, S. J., Steiner, R., "Polymer gel electrolyte supported with microporous polyolefin membranes for lithium ion polymer battery," *Solid State Ionics* Vol. 148, 2002, pp. 443-449.

¹⁵Jaworek, A., "Electrospray droplet sources for thin film deposition," *J. Mater. Sci.* Vol. 42, 2007, pp. 266-297.

¹⁶Bock, N., Dargaville, T. R., Woodruff, M. A., "Electrospraying of polymers with therapeutic molecules: State of the art," *Prog. Polym. Sci.* Vol. 37, 2012, pp. 1510-1551.

¹⁷Huang, G. Jian, J. B. Delisio, H. Wang, M. R. Zachariah, "Electrospray Deposition of Energetic Polymer Nanocomposites with High Mass Particle Loadings: A Prelude to 3D Printing of Rocket Motors," *Adv. Eng. Mater.* Vol. 17, 2015, pp. 95-101.

¹⁸Li, X., Guerieri, P., Zhou, W., Huang, C., Zachariah, M. R., "Direct Deposit Laminate Nanocomposites with Enhanced Propellant Properties," *ACS Appl. Mater. Interfaces*, Vol. 7, 2015, pp. 9103-9109.